Received: 10 March 2020 | Revised: 17 May 2020 | Accepted: 22 May 2020

DOI: 10.1002/ardp.202000075

Check for updates

FULL PAPER

DPhG ARCH PHARM Archiv der Pharmazie

N-Substituted pyrimidinethione and acetophenone derivatives as a new therapeutic approach in diabetes

Parham Taslimi[1] | Afsun Sujayev[2] | Muhammet Karaman[3] | Gunel Maharramova[2] | Nastaran Sadeghian[4] | Sabiya Osmanova[2] | Sabira Sardarova[2] | Nargiz Majdi[2] | Handan U. Ozel[5] | İlhami Gulcin[4]

[1]Department of Biotechnology, Faculty of Science, Bartin University, Bartin, Turkey

[2]Laboratory of Theoretical Bases of Synthesis and Action Mechanism of Additives, Institute of Chemistry of Additives, Azerbaijan National Academy of Sciences, Baku, Azerbaijan

[3]Department of Molecular Biology and Genetics, Faculty of Arts and Science, Kilis 7 Aralik University, Kilis, Turkey

[4]Department of Chemistry, Faculty of Sciences, Ataturk University, Erzurum, Turkey

[5]Department of Environmental Engineering, Faculty of Engineering, Bartin University, Bartin, Turkey

Correspondence
Parham Taslimi, Department of Biotechnology, Faculty of Science, Bartin University, 74100 Bartin, Turkey.
Email: parham_taslimi_un@yahoo.com; ptaslimi@bartin.edu.tr

Abstract

In this study, compounds with 4-hydroxybutyl, 4-phenyl, 5-carboxylate, and pyrimidine moieties were determined as α-glycosidase inhibitors. *N*-Substituted pyrimidinethione and acetophenone derivatives (**A1**–**A5**, **B1**–**B11**, and **C1**–**C11**) were good inhibitors of the α-glycosidase enzyme, with K_i values in the range of 104.27 ± 15.75 to 1,004.25 ± 100.43 nM. Among them, compound **B7** was recorded as the best inhibitor, with a K_i of 104.27 ± 15.75 nM against α-glycosidase. In silico studies were carried out to clarify the binding affinity and interaction mode of the compounds with the best inhibition score against α-glycosidase from *Saccharomyces cerevisiae*. Compounds **B7** (*S*) and **B11** (*R*) exhibited a good binding affinity with docking scores of −8.608 and 8.582 kcal/mol, respectively. The docking results also showed that the 4-hydroxybutyl and pyrimidinethione moieties play a key role in *S. cerevisiae* and human α-glycosidase inhibition.

KEYWORDS

acetophenone, diabetes mellitus, molecular docking, *N*-substituted pyrimidinethione, α-glycosidase

1 | INTRODUCTION

Heterocyclic compounds are the main class combinations with a large spectrum of pharmacological and biological activities.[1] Recently, it has been observed that dihydropyrimidines with functional values are the compounds that have biological activities including antiviral and antibacterial properties.[2,3] However, while analyzing the most recent literature, it becomes clear that the formulation of heterocyclic compound of thiourea by three-component condensation reactions mainly covers the synthesis of dihydropyrimidinethiones.[4,5] The reaction products of aldehydes and ketones with thioglycolic acid are compounds containing functional groups such as carboxyl and hydroxyl groups, which are receiving great attention. These compounds can be valuable synthons for the synthesis of different esters,[6,7] amides, and heterocyclic compounds.[8] Amides of organic acids are used as plasticizers of industrial and intermediate products in the synthesis of dyes, as well as sulfa drugs in medicine.[9]

α-Glycosidase is a digestive enzyme that hydrolyzes carbohydrate molecules including disaccharides and starches to generate more metabolically available sugars in the course of catabolic metabolism.[10,11] Indeed, it can functionally hydrolyze carbohydrate molecules. The α-glycosidase enzyme is distinct from β-glycosidase, which cleaves glycosidic bonds. It is generally well recorded that α-glycosidase is associated with type 2 diabetes mellitus (T2DM) due to the fact that the high activity of this enzyme enhances plasma glucose levels, which, in turn, affect glucose absorption in T2DM.[12] Thus, several studies regarding α-glycosidase inhibition and the development of its inhibitors have been reported and also conducted due to interest in the treatment of T2DM via downregulation of α-glycosidase activity (Figure 1). Thus, various α-glycosidase inhibitors

 © 2020 Deutsche Pharmazeutische Gesellschaft

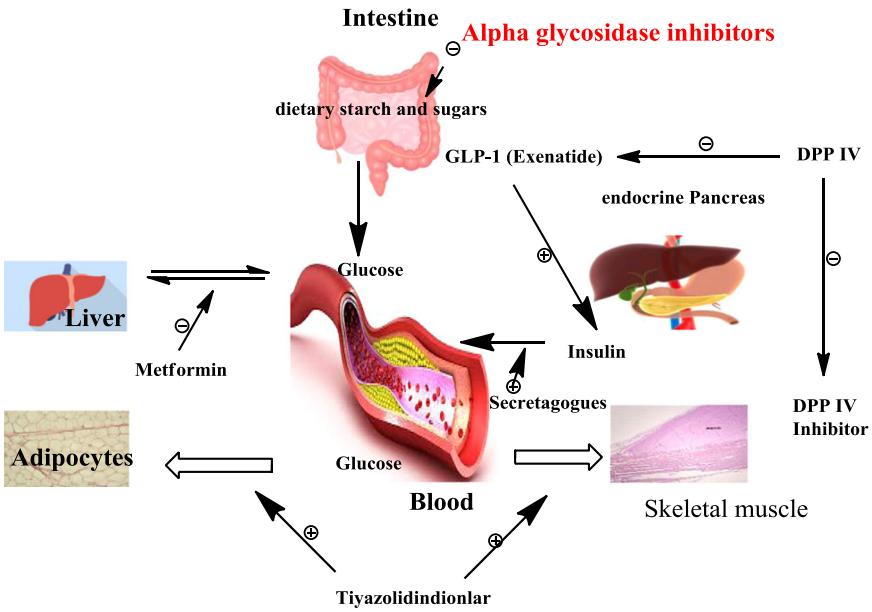

FIGURE 1 The mechanism of action of α-glycosidase enzyme inhibitors

such as acarbose, voglibose, and miglitol have been highlighted and mostly addressed in the clinical setting.[13,14]

This study aimed at investigating the α-glycosidase enzyme inhibition of *N*-substituted pyrimidinethione and acetophenone derivatives (**A1**–**A5**, **B1**–**B11**, and **C1**–**C11**) on α-glycosidase enzyme. Also, the study aimed to understand a possible inhibition mechanism of the most active compounds against the enzyme using molecular docking simulation.

2 | RESULTS AND DISCUSSION

2.1 | Chemistry

First, in the presence of trifluoroacetic acid (TFA), an efficient method for the synthesis of tetra(hexa)hydropyrimidinethione-carboxylates (**A1**–**A5**) has been used on the basis of three-component condensation of thiourea with different aldehydes and β-diketones derivatives[15] (Scheme 1).

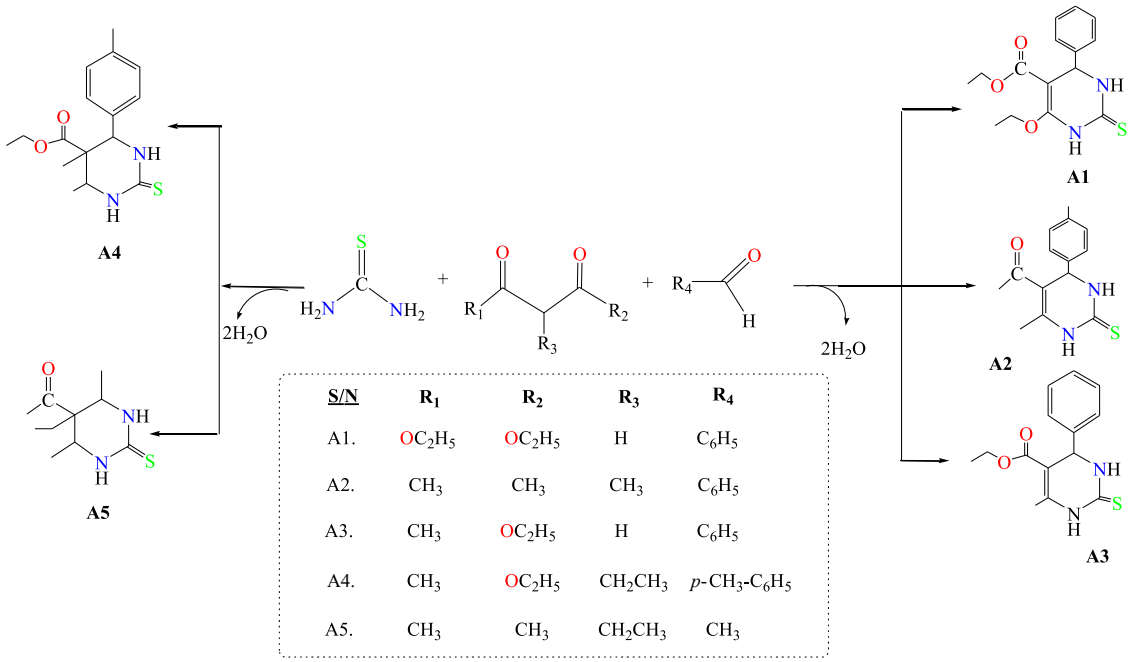

S/N	R_1	R_2	R_3	R_4
A1.	OC_2H_5	OC_2H_5	H	C_6H_5
A2.	CH_3	CH_3	CH_3	C_6H_5
A3.	CH_3	OC_2H_5	H	C_6H_5
A4.	CH_3	OC_2H_5	CH_2CH_3	*p*-CH_3-C_6H_5
A5.	CH_3	CH_3	CH_2CH_3	CH_3

SCHEME 1 The synthesis of cyclic thioureas (**A1**–**A5**)

Various aldehydes and active methylene compounds with thiourea have been elaborated in the effective method of synthesis of dihydropyrimidinethiones, and their conversions have been carried out. Nowadays, many methods have been reported for the preparation of tetra(hexa)hydropyrimidinethiones. Taking this into consideration, tetrahydropyrimidinethiones were synthesized by Biginelli reaction. The nucleophilic displacement reaction occurred between 1,2-epoxypropane and 1,2-epoxybutane, and pyrimidinethiones and new compounds were obtained (**B1**–**B6**). By this known method, the mutual influence reaction was conducted between tetrahydropyrimidinethiones and 4-chlorobutanol-1 as a nucleophile. Triethylamine is used as a catalyst. As a result of the reaction, compounds **B7**–**B11** were synthesized with 65–70% yield[16] (Scheme 2).

The thiolation reaction was performed in a benzene solution at 80°C with *p*-substituted ketones and mercaptoacetic acid in a molar ratio of 1:4 in the presence of a catalytic amount of toluene sulfonic acids. According to the reaction of mutilation of acetophenone and some of its *p*-substituted derivatives 1,1-bis-(carboxymethylthio)-1-arylethanes were obtained. It was found that during the reaction, 1-hydroxy-1-(carboxymethylthio)-1-arylethanes spontaneously cyclized to form 2-aryl-2-methyl-1,3-oxathiolane-5-ones. A direct amidation reaction of 1,1-bis-(carboxymethylthio)-1-arylethanes with primary amines was conducted[17] (Scheme 3).

2.2 | Enzyme results

For α-glycosidase, *N*-substituted pyrimidinethione and acetophenone derivatives (**A1**–**A5**, **B1**–**B11**, and **C1**–**C11**) have IC_{50} values in the range of 94.16–1,005.24 nM and K_i values in the range of 104.27 ± 15.75 to 1,004.25 ± 100.43 nM (Table 1 and Figure 2). The results clearly show that all of the derivatives have inhibitory effects on α-glycosidase as efficient as acarbose (IC_{50}: 22.8 μM), a standard α-glycosidase inhibitor.[18] In fact, the most effective K_i values were observed for **B7** and **B11**, with K_i values of 104.27 ± 15.75 and 236.32 ± 24.74 nM, respectively. However, the weakest inhibition was obtained with compounds **A5** and **A4**, with K_i values of 1,004.25 ± 100.43 and 989.95 ± 135.21 nM, respectively. Group **B** showed better results than Groups **A** and **C**. Compounds **B1**–**B11** have IC_{50} values in the range of 94.16–504.28 nM and K_i values of 104.27 ± 15.75 to 605.23 ± 93.08 nM. It was known that heterocyclic compounds have α-glycosidase inhibition profiles. In this context, Natori and colleagues found that 1-*C*-butyl-L-arabino-iminofuranose had potent inhibitory effects against α-glycosidase enzymes.[19] In a recent study, it was reported that a novel Ag-N-heterocyclic carbene complex had α-glycosidase inhibition properties.[20] Some inhibitors like acarbose, miglitol, and voglibose are commercial α-glycosidase inhibitors, which are considered as the first-line therapy for diabetic individuals with postprandial hyperglycemia. Although these compounds are effective in attenuating the rise in the blood sugar level in

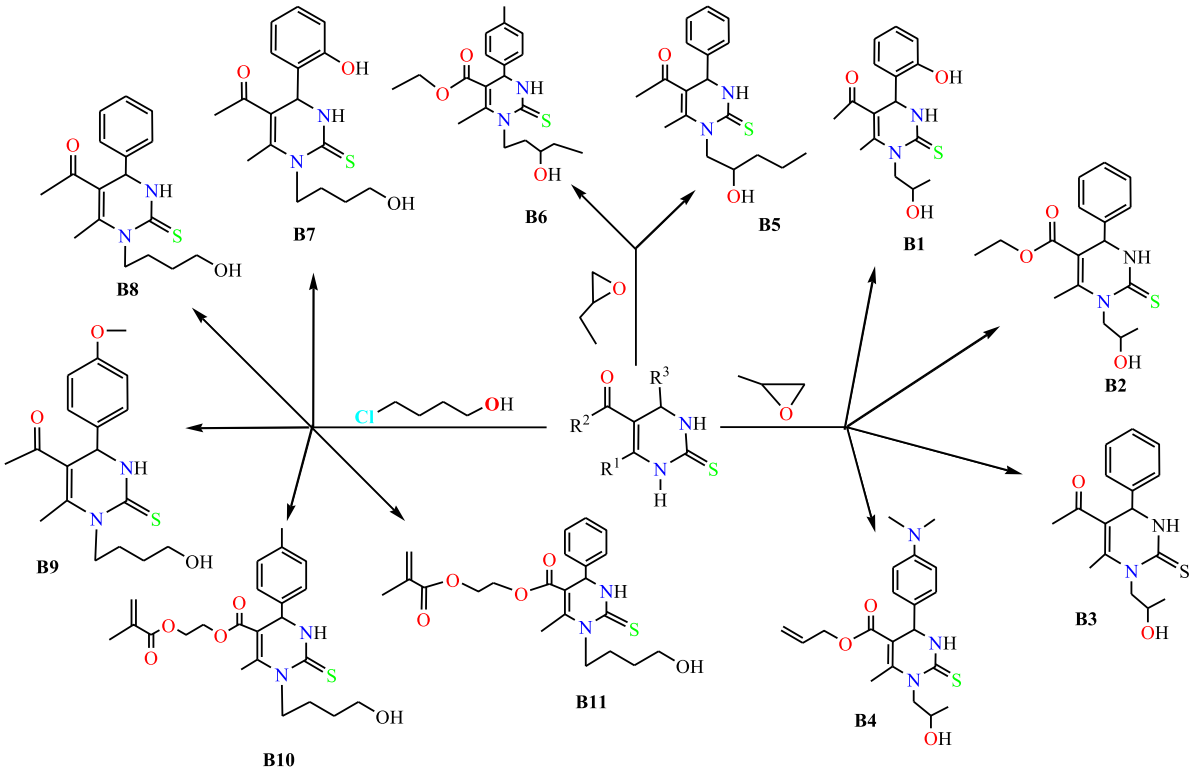

SCHEME 2 The synthesis of derivatives of new pyrimidinethiones (**B1**–**B11**)

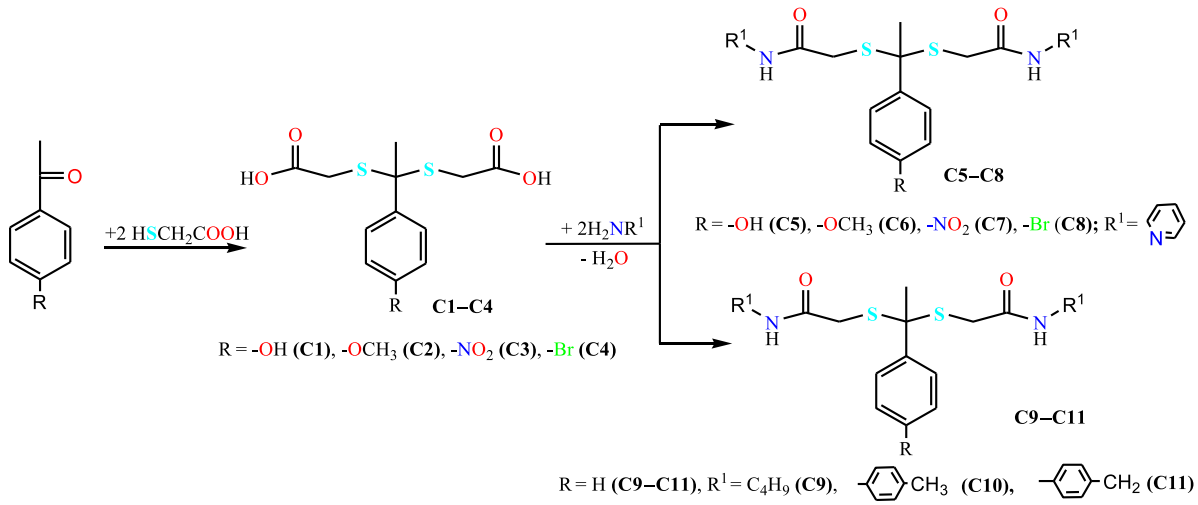

SCHEME 3 The synthesis of amides of 1,1-bis-(carboxymethylthio)-1-arylethanes (**C1**–**C11**)

patients, unfortunately, their continuous use may lead to undesirable side effects, for example, adverse gastrointestinal symptoms and liver toxicity.[21,22]

In this study, the enzyme inhibition of *N*-substituted pyrimidinethione and acetophenone derivatives (**A1**–**A5**, **B1**–**B11**, and **C1**–**C11**) against α-glycosidase enzyme was analyzed, and also the results were calculated and evaluated. The α-glycosidase enzyme is involved in many biological functions associated with several diseases: (a) It participates in tumor metastasis via cellular interaction with collagen type I, II, and IV; (b) α-glycosidase enzyme inhibition effectively decreases the risk of colorectal cancer and cerebrovascular events in T2DM; and (c) an autosomal recessive disturbance affecting α-glycosidase causes Pompe disease. Thus, α-glycosidase has an extensive range of potential effects, which include aiding in the extension of an inhibitor of α-glycosidase for treating T2DM.[23,24] The α-glycosidase inhibitors act against these metabolic enzymes in the gut tissue, slowing down the liberation of D-glucose from dietary complex carbohydrate molecules that lower available glucose for absorption. Indeed, they have beneficial effects, as they delay the progression of diabetes and decrease postprandial blood glucose in treating prediabetic conditions.[22,25]

2.3 | In silico studies

In silico studies were carried out for clarifying binding affinity and interaction mode of the compounds with the best inhibition score against the α-glycosidase enzyme from *Saccharomyces cerevisiae*. To understand binding affinity and interaction mode of the compounds, the compounds were additionally docked into the catalytic active site of the *S. cerevisiae* and human lysosomal α-glycosidase enzyme. The inhibitory effect of stereoisomers of the compounds on α-glycosidase enzyme was evaluated with both α-glycosidase from *S. cerevisiae* and human lysosomal α-glycosidase receptors. Before performing docking studies, we tested the druglikeness properties of synthesized compounds. After QikProb calculation, we considered the number of reactive functional groups, molecular weight, hydrogen bond donor and acceptor, octanol/water partition coefficient, IC_{50} value for blockage of HERG K^+ channels, Caco-2 cell permeability, brain/blood partition coefficient, Madin–Darby canine kidney (MDCK) cell permeability, and human oral absorption rate of the compounds for evaluation of druglikeness properties. Druglikeness results of compounds **B7** and **B11** have also been shown in Table 2. The results have indicated that both compounds are capable of displaying good drug properties, because they were nontoxic, highly permeable across membrane, and well adsorbable. **A** and **B** compounds have exhibited similar physical properties. However, unlike others, most of **C** compounds did not have good physical properties on the basis of blockage of HERG K^+ channels, Caco-2, and MDCK cells membrane permeability, and human oral absorption.

We identified the binding site of *S. cerevisiae* α-glycosidase and human lysosomal α-glycosidase receptors before docking process of **B7** and **B11**, which exhibited best inhibitory effect during in vitro experiment. We evaluated catalytic active site and druggable site properties of the binding sites on the basis of SiteScore and DScore. The binding sites of *S. cerevisiae* α-glycosidase and human lysosomal α-glycosidase receptors have SiteScore values of 1.136 and 0.907, respectively, and DScore values of 1.024 and 0.802, respectively. The scores have shown quite good catalytic active site and druggable site properties of the predicted binding site. The predicted catalytic active sites have been used for evaluating the best poses of **B7** and **B11** compounds, as seen in Figure 3.

We first tested the reliability of induced-fit docking technique. For this purpose, we docked cocrystallized ligands, which are D-glucose and acarbose, into predicted catalytic active site of *S. cerevisiae* α-glycosidase and human lysosomal α-glycosidase receptors, and subsequently analyzed the binding position and root mean square deviation (RMSD) value of redocking ligands. RMSD values were calculated as 1.651 and 1.772 Å for *S. cerevisiae* α-glycosidase and human lysosomal α-glycosidase receptors, respectively, with

TABLE 1 The inhibition results of *N*-substituted pyrimidinethione and acetophenone derivatives (**A1**–**A5**, **B1**–**B11**, and **C1**–**C11**) against the α-glycosidase enzyme

Compounds	IC_{50} values (nM)	R^2	K_i values (nM)
A1	945.03	0.9345	988.23 ± 94.34
A2	902.63	0.9813	974.11 ± 105.50
A3	734.88	0.9104	805.25 ± 84.55
A4	1,005.24	0.9893	989.95 ± 135.21
A5	941.62	0.9424	1,004.25 ± 100.43
B1	473.16	0.9821	506.95 ± 57.32
B2	402.70	0.9683	465.13 ± 35.94
B3	283.04	0.9611	325.82 ± 52.63
B4	489.11	0.9904	605.23 ± 93.08
B5	504.28	0.9732	483.27 ± 52.05
B6	416.10	0.9808	402.54 ± 24.88
B7	94.16	0.9527	104.27 ± 15.75
B8	394.37	0.9623	458.43 ± 47.13
B9	400.24	0.9842	495.14 ± 42.30
B10	473.68	0.9011	546.83 ± 100.32
B11	198.15	0.9384	236.32 ± 24.74
C1	602.10	0.9931	705.30 ± 40.82
C2	638.16	0.9642	623.11 ± 74.03
C3	724.24	0.9730	811.42 ± 125.32
C4	624.03	0.9882	680.33 ± 91.26
C5	538.41	0.9297	598.12 ± 41.17
C6	688.93	0.9688	745.33 ± 103.21
C7	396.16	0.9180	361.27 ± 37.96
C8	605.30	0.9724	734.21 ± 78.36
C9	695.14	0.9821	750.30 ± 95.03
C10	734.22	0.9903	730.73 ± 38.94
C11	615.83	0.9068	657.11 ± 153.78
ACR[a]	22,800	–	12,600 ± 780

[a]Acarbose (ACR) was used as a standard inhibitor for the α-glycosidase enzyme.[18]

atom pair method. The RMSD values have indicated that the docking technique was quite reliable. The best pose of cocrystallized and redocked ligands is shown in Figure 4.

After the reliability of the docking technique has been identified, we have carried out docking process of compounds **B7** and **B11** with best inhibition score. To evaluate binding affinity and the possible inhibition mechanism of the compounds, docking results have been evaluated on the basis of docking score and binding mode. We also compared docking scores and binding modes of the compounds and standard inhibitors of *S. cerevisiae* α-glycosidase and human lysosomal α-glycosidase receptors. Ligands with highest glide Emodel score in the negative direction have been selected as best-posed ligands, and their binding affinity against the receptors is presented in Table 3. According to the binding affinity scores, the compounds very well interacted with *S. cerevisiae* α-glycosidase receptor. Besides, the compounds have more high docking and Glide score in the negative direction from the standard inhibitor. The binding affinity of the compounds against the human lysosomal α-glycosidase receptor was slightly weak, compared with acarbose, which is a standard inhibitor. The best binding affinity score for compound **B7** was obtained with (*S*)-stereoisomer for both *S. cerevisiae* α-glycosidase and human lysosomal α-glycosidase receptors. The best binding affinity score for compound **B11** was contrarily obtained with (*R*)-isomer. To clarify the possible inhibition mechanism of the inhibitors against *S. cerevisiae* and human α-glycosidase receptors, 2D and 3D detailed binding modes of best-posed ligands were analyzed and presented in Figure 5.

4-Hydroxybutyl moiety directly formed hydrogen bonds with Asp69 and Arh442 residues and formed a hydrogen bond with Arg446 residue via a water bridge. The hydroxyphenyl moiety formed hydrogen bonds with Arg315 and Glu411 residues and also interacted with Tyr158 residue through π–π stacking. Also, the tetrahydropyrimidine moiety formed a hydrogen bond with Gln353 residue of *S. cerevisiae* α-glycosidase receptor. Besides, compound **B7** (*S*) formed an aromatic hydrogen bond with Gln279 residue, as seen in Figure 5A-a. The (*R*)-stereoisomer of the compound formed hydrogen bonds with Tyr158 and Asn455 residues via 4-hydroxybutyl moiety and with Arg213 and Asp352 residues via hydroxyphenyl moiety (Figure S2A-a). The 4-hydroxybutyl, 4-phenyl, 5-carboxylate, and pyrimidine moieties of compound **B11** (*R*) were responsible for inhibition of the enzyme due to many interactions with residues of *S. cerevisiae* α-glycosidase enzyme. Whereas the 4-phenyl moiety formed a π–π stacking interaction with Phe303 residue, the other moieties formed hydrogen bonds with catalytic active site residues. The 4-hydroxybutyl moiety interacted with Arg213 and Asp352, 5-carboxylate interacted with Arg315, and pyrimidine moiety interacted with Glu411 residues of the receptor. Moreover, the compound formed an aromatic hydrogen bond with Hie280 (Hie: histidine with hydrogen on the epsilon nitrogen), Phe314, Asp352, and Glu411 residues, as seen in Figure 5A-b. The compounds also interacted with hydrophobic residue via the 4-phenyl moiety, as seen in Figure 3a,b. The (*S*)-stereoisomer of the compound has interacted with more active site residues through a hydrogen bond. Nevertheless, the interaction is not with key residues in the active site. Also, it has lost interaction with gatekeeper residues, Phe303 (Figure S2A-b).

The 4-hydroxybutyl and hydroxyphenyl moieties of the compound **B7** (*S*) interacted with catalytic active site residues of the human lysosomal α-glycosidase receptor. The 4-hydroxybutyl moiety formed three hydrogen bonds with Ser676, Leu677, and Leu678 residues. The hydroxyphenyl moiety formed a hydrogen bond with Asp616 residue. Besides, 6-methyl-2-thioxo-1,2,3,4-tetrahydropyrimidine moiety interacted with Phe649 residue through π–π stacking, as seen in Figure 5B-a. The (*R*)-stereoisomer of the compound formed hydrogen bonds with Asp518 and Gly651 residues and π–π stacking interactions with Trp376 and Phe649 residues. Moreover, the compound formed an aromatic hydrogen bond with Asp404 and Trp481 residues (Figure S2B-a).

The 4-hydroxybutyl, thione and pyrimidine moieties of compound **B11** (*R*) formed a hydrogen bond with Asp518, Arg600, and Asp616, respectively. The 4-hydroxybutyl moiety also formed a

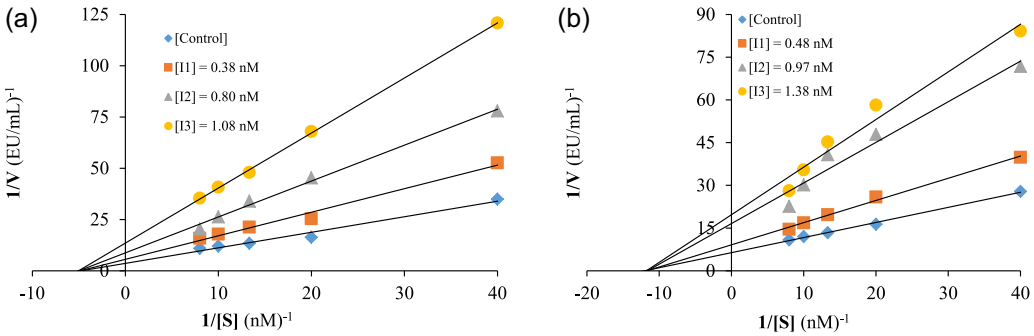

FIGURE 2 Determination of Lineweaver-Burk graphs for excellent inhibitors of α-glycosidase enzyme (**a**: **B7** and **b: B11**)

TABLE 2 Pharmaceutical properties of the *N*-substituted pyrimidinethione and acetophenone derivatives

Compound	rtvFG	MW	DHB	AHB	logPo/w	logHERG	Caco	logBB	PMDCK	% Hum. oral abs.
A1	1	306.379	0.000	2.500	4.470	−4.667	2,071.235	−0.137	3,010.318	100.000
A2	0	260.353	0.000	2.500	3.792	−4.461	2,257.208	0.083	3,311.506	100.000
A3	1	276.353	0.000	2.500	3.992	−4.801	1,727.031	−0.105	2,479.503	100.000
A4	0	306.422	0.000	2.500	4.655	−4.047	3,364.389	0.187	4,520.368	100.000
A5	0	214.325	0.000	2.500	2.792	−2.859	3,345.171	0.244	4,953.326	100.000
B1	0	320.406	2.000	5.950	2.748	−4.177	1,213.220	−0.404	1,360.712	100.000
B2	1	334.432	1.000	5.200	3.592	−4.849	1,243.202	−0.494	1,266.003	100.000
B3	0	304.406	1.000	5.200	3.032	−4.139	1,364.591	−0.301	1,514.714	100.000
B4	1	389.512	1.000	6.200	4.308	−4.933	1,289.362	−0.638	1,376.302	100.000
B5	0	318.433	1.000	5.200	3.585	−4.561	1,819.753	−0.279	2,128.634	100.000
B6	1	376.513	1.000	5.200	4.799	−5.130	1,558.831	−0.574	1,721.984	100.000
B7	0	334.432	2.000	5.950	2.938	−4.890	658.875	−0.885	683.585	94.597
B8	0	318.433	1.000	5.200	3.334	−4.596	937.555	−0.629	999.946	100.000
B9	0	348.459	1.000	5.950	3.390	−4.570	811.860	−0.786	854.668	100.000
B10	1	446.560	1.000	7.200	4.563	−5.640	314.450	−1.619	305.570	100.000
B11	2	432.534	1.000	7.200	4.471	−5.837	488.697	−1.361	492.520	100.000
C1	0	302.360	3.000	5.750	1.664	−0.684	1.558	−2.285	1.252	40.131
C2	0	316.386	2.000	5.750	2.474	−0.673	5.132	−1.812	4.557	54.144
C3	0	331.358	2.000	6.000	1.694	−0.763	0.620	−2.730	0.463	33.142
C4	0	365.256	2.000	5.000	2.927	−0.772	5.176	−1.574	12.207	56.860
C5	0	454.561	2.000	8.750	3.598	−7.874	186.683	−2.083	133.922	88.662
C6	0	468.588	2.000	8.750	3.954	−6.225	974.410	−0.975	829.040	100.000
C7	0	483.559	2.000	9.000	3.617	−7.801	74.005	−2.589	49.261	81.582
C8	0	517.457	2.000	8.000	4.915	−7.796	667.738	−1.131	1,456.136	93.319
C9	0	396.605	2.000	6.000	3.178	−2.015	529.141	−0.964	1,062.773	94.298
C10	0	464.639	2.000	6.000	6.154	−7.903	1,183.134	−1.057	1,005.316	100.000
C11	0	464.639	2.000	6.000	5.004	−5.454	372.246	−1.178	934.025	89.302

Abbreviations: AHB, number of hydrogen bond acceptors; Caco, Caco-2 cell membrane permeability; DHB, number of hydrogen bond donors; logBB, brain/blood partition coefficient; logHERG, IC_{50} value for blockage of HERG K^+ channels; logPo/w, octanol/water partition coefficient; MW, molecular weight; PMDCK, MDCK cell permeability in nm/s; rtvFG, reactive group (tox); % Hum. oral abs., qualitative human oral absorption.

hydrogen bond with a water molecule in the catalytic active site. The 4-phenyl moiety interacted with Arg600 residue through π−cation. The 4-phenyl moiety also formed aromatic hydrogen bonds with Trp481 via water molecule and Asp616 residues, as seen in Figure 5B-b. Figure 3c,d has shown that the compounds less interacted with hydrophobic residues in comparison with *S. cerevisiae* α-glycosidase receptor. In contrast to the (*R*)-stereoisomer, the (*S*)-stereoisomer of the compound interacted with the hydrophobic residues Trp376, Leu677, and lLeu678 (Figure S2B-b).

Tetrahydropyrimidine, 4-hydroxybutyl, and hydroxyphenyl moieties of compound **B7** (*S*) play a key role in the inhibition of *S. cerevisiae* α-glycosidase receptors. These binding modes have shown that the

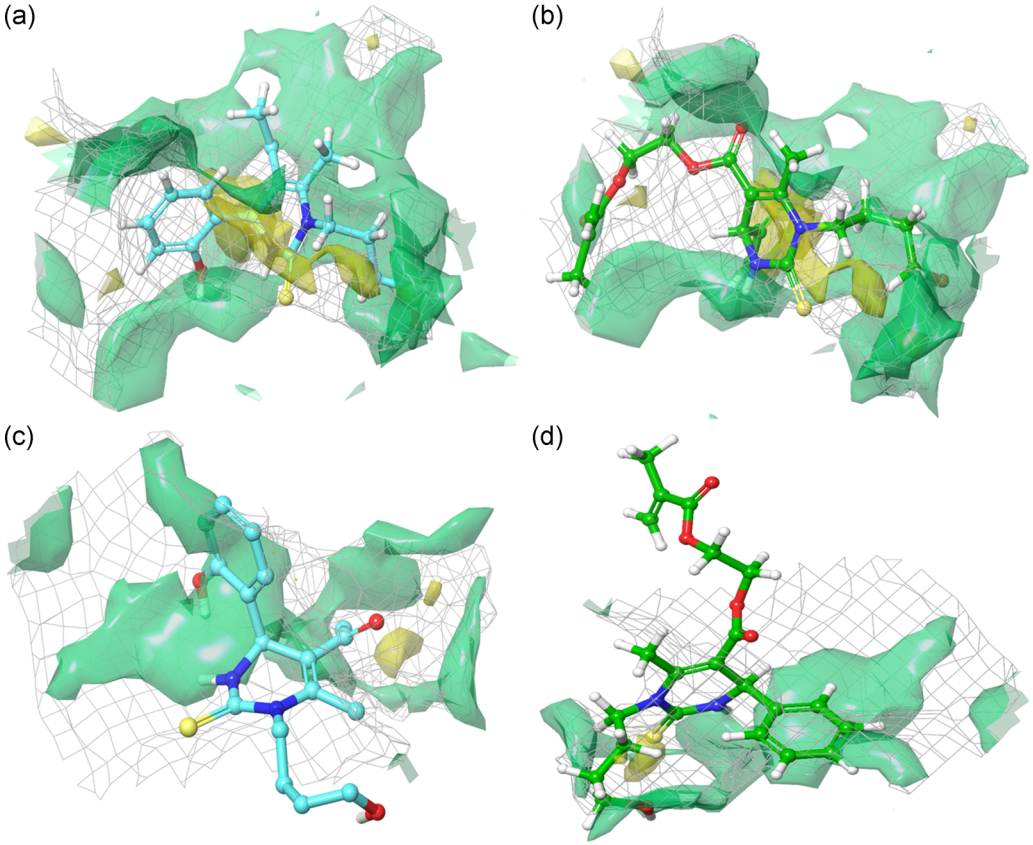

FIGURE 3 The predicted catalytic active sites of the α-glycosidase receptors. *Saccharomyces cerevisiae* α-glycosidase is presented in the top panel: (a) B7 (*S*) and (b) B11 (*R*). Human α-glycosidase is presented in the bottom panel: (c) B7 (*S*) and (d) B11 (*R*). The catalytic active site has been represented as a gray mesh surface, the hydrophobic site has been represented as a yellow bubble, and the hydrophilic site has been represented as a green bubble

compounds located in the catalytic active site of the receptors exhibited a similar interaction with acarbose, as seen in Figure S1-a. Yamamoto et al.[26] have expressed that Asp69 and Asp352 residues interacted with substrate, and Arg213, Asp352, and Arg446 residues interacted with water molecules in the catalytic active site, and they have played a crucial role. Other publications reported by Yamamoto et al.[27] indicated that Tyr158, Phe303, Glu411, and Asp442 residues were important for the enzyme activity. Besides, it has been reported that tetrazolo[1,5-*a*]-pyrimidine derivatives,[28] pyrimidine-2,4,6-trione derivatives,[29] coumarin–iminothiazolidinone hybrids,[30] and diarylimidazole-1,2,3-triazole hybrids[31] inhibited the enzyme by interacting with catalytic active site residue. However, the inhibitors mostly interacted with hydrophobic residues in catalytic active sites of the enzyme due to their aromatic ring moieties. According to our docking results, the

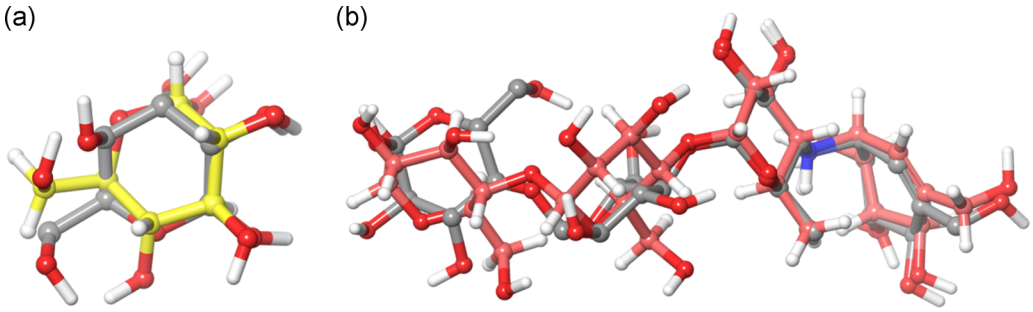

FIGURE 4 Induced-fit docking technique was tested calculating RMSD value between cocrystallized ligand and best-pose of redocked ligand. (a) D-Glucose was redocked for *Saccharomyces cerevisiae* α-glycosidase receptor and (b) acarbose was redocked for human α-glycosidase receptor. Cocrystalized D-glucose was represented with yellow ball–stick, cocrystallized acarbose was represented with faded-red ball-stick and re-docked ligands were represented with grey ball-stick

TABLE 3 Binding affinity scores (kcal/mol) of **B7** and **B11** stereoisomers in the catalytic sites of the α-glycosidase receptors

Compounds	*Saccharomyces cerevisiae* α-glycosidase			Human α-glycosidase		
	Docking score	Glide score	Glide Emodel	Docking score	Glide score	Glide Emodel
B7 (*S*)	−8.608	−8.610	−88.520	−6.065	−6.065	−56.393
B7 (*R*)	−7.378	−7.379	−74.148	−5.559	−5.561	−60.102
B11 (*S*)	−8.368	−8.368	−88.086	−5.861	−5.861	−62.267
B11 (*R*)	−8.582	−8.582	−95.083	−6.163	−6.163	−70.314
ACR[a]	−7.962	−8.290	−140.803	−7.334	−7.662	−112.995

[a]Acarbose (ACR) was used as a standard inhibitor for the α-glycosidase enzyme.[18]

(*S*)-stereoisomer of compound **B7** and the (*R*)-stereoisomer of compound **B11** have mainly interacted with mentioned residues, especially Tyr158, Phe303, and Glu411. However, other stereoisomers of the compounds interacted with less important active site residues due to conformational changing. The differences lead to losing π−π stacking interaction with gatekeeper residues, Tyr158 and Phe303.

On the other side, interactions between the compounds and residues of human lysosomal α-glycosidase receptor were less than interactions between the compounds and residues *S. cerevisiae* α-glycosidase enzyme. The human receptor's active site is stabilized with H-bonds between side chains of Asp404, Asp518, Arg600, Asp616, and His674 residues. A hydrophobic contact between Trp376, Ile441, Trp516, Met519, Trp613, and Phe649 residues results in the stabilization.[32] Taj et al.[33] have reported that pyrazolobenzothiazine 5,5-dioxide derivatives inhibit Asp203, Asp542, Asp327, His600, and Arg526 residues of human maltase-glucoamylase enzyme that is related to the human α-glycosidase. In our previous study, we have explained that imidazolinium chloride salt potently inhibited the human maltase-glucoamylase enzyme by interacting with Asp542 and Gln603 residues through a salt bridge and hydrogen bond, respectively.[34] According to the binding modes of the (*S*)-stereoisomer of compound **B7** and the (*R*)-stereoisomer of compound **B11**, they interacted with Arg600, Asp616, and Asp512 residues, which

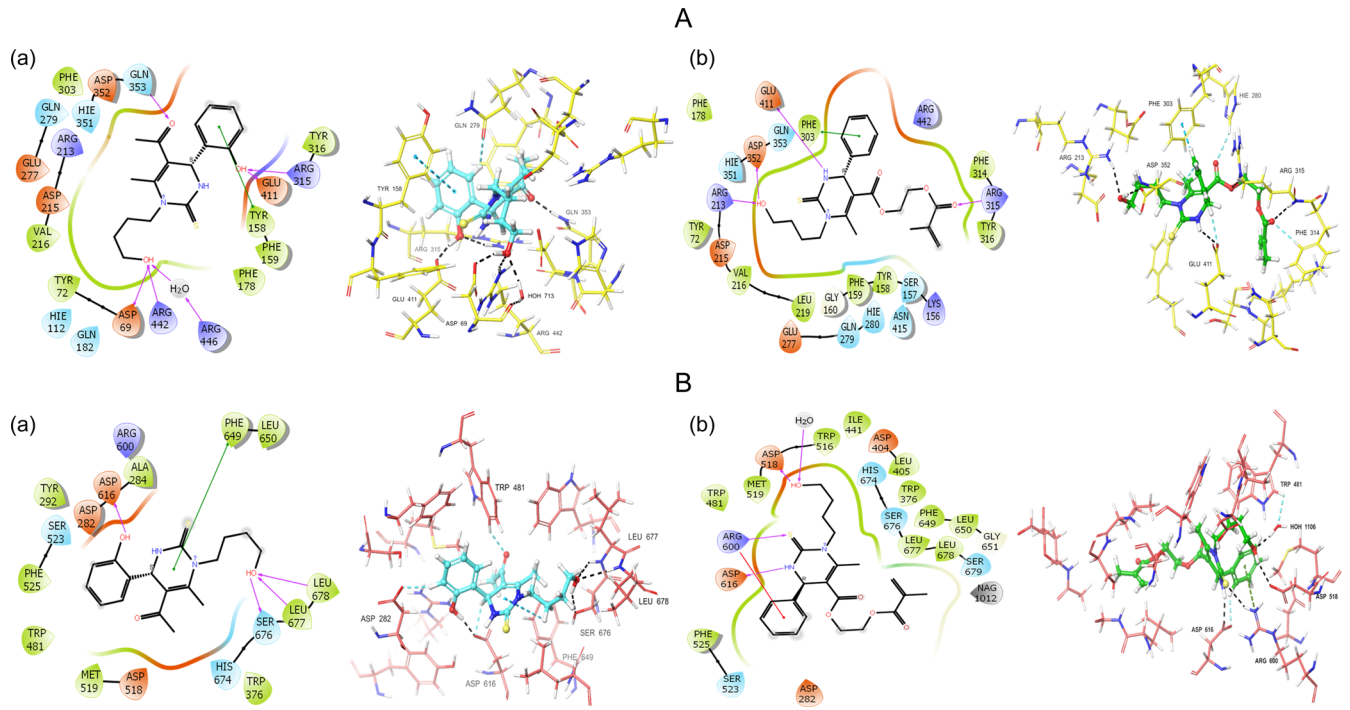

FIGURE 5 (A) 2D and 3D interaction diagrams of the compounds complexed with *Saccharomyces cerevisiae* α-glycosidase receptor. The receptor structure was represented as a yellow ribbon model, amino acid residues were represented as a thick tube model, (a) compound **B7** (*S*) was represented as a turquoise ball–stick model, and (b) compound **B11** (*S*) was represented as a green ball–stick model. (B) 2D and 3D interaction diagrams of the compounds complexed with human α-glucosidase receptor. The receptor structure was represented as a faded red ribbon model, amino acid residues were represented as a thick tube model, (a) compound **B7** (*R*) was represented as a turquoise ball–stick model, and (b) compound **B11** (*R*) was represented as a green ball–stick model

are critical for enzyme catalytic activity. However, other stereoisomers of the compounds have lost interaction with the critical residues as with the other enzyme. The 4-hydroxybutyl and pyrimidinethiones moieties played a key role in *S. cerevisiae* and human α-glycosidase inhibition.

3 | CONCLUSION

These synthesized novel compounds, **B7** and **B11**, have shown efficient inhibitory actions; hence, they can be used as a leading candidate for initiation of effective α-glycosidase inhibitors. The molecular docking studies on the enzymes have also shown that the most active compounds **B7** (*S*) and **B11** (*R*) have strongly bound to the catalytic active site of the enzyme.

4 | EXPERIMENTAL

4.1 | Chemistry

4.1.1 | Synthesis of cyclic thioureas (A1–A5)

The TFA, a new effective synthesis method of tetra(hexa) hydropyrimidinethione-carboxylates (**A1**–**A5**), has been employed in this study. The three-component condensation reactions were performed for 2.5–3.0 hr at 60–75°C.[15]

4.1.2 | Synthesis of derivatives of new pyrimidinethiones (B1–B11)

Pyrimidinethiones (0.02 mol) were dissolved in 2:1 ratio of acetylacetone (12 ml) and ethyl alcohol (5 ml); also, 1,2-epoxypropane (1,2-epoxybutane) (0.02 mol) was added to this mixture drop by drop. After being dissolved, it was stirred for 30 min, and then 20 mg $AlCl_3$ catalyst was added to it. Then, it was mixed and heated at 60–65°C. The synthesis of these compounds was described in detail in the previous study.[16] After the completion of the reaction, the mixture is cooled, purified by means of recrystallization with ethanol, and dried.

4.1.3 | The amides of 1,1-bis-(carboxymethylthio)-1-arylethanes derivatives (C1–C11)

The synthesis of these compounds was recorded in detail in the previous study.[17] All the synthesized compounds (**A1**–**A5**, **B1**–**B11**, and **C1**–**C11**) were filtered and dried in dichloromethane crystallized from ethyl alcohol. All reagents were purchased and used without further purification. Glassware was dried before use. Compounds were purified by dry flash chromatography using silica 60, <0063 mm, and water pump vacuum or by flash chromatography using silica 60 Å, 230–400 mesh as stationary phases. Thin-layer chromatography plates (silica gel 60 F_{254}) were visualized either with a UV lamp or iodine. Their structure was confirmed by spectral and physicochemical methods, such as ^{1}H and ^{13}C nuclear magnetic resonance spectroscopy.[15–17]

The InChI keys of the investigated compounds, together with some biological activity data, are provided as Supporting Information Data.

4.2 | α-Glycosidase inhibition assay

The inhibitory effect of the *N*-substituted pyrimidinethione and acetophenone derivatives (**A1**–**A5**, **B1**–**B11**, and **C1**–**C11**) on the α-glycosidase enzyme activity was assayed using *p*-nitrophenyl-D-glycopyranoside (*p*-NPG) substrate, according to the assay of Tao et al.[18] as described previously.[35–37] First, 200 µl of phosphate buffer was mixed with 40 µl of the homogenate solution in a phosphate-buffered solution (PBS; 0.15 U/ml, pH 7.4). Also, 50 µl of *p*-NPG in a PBS (5 mM, pH 7.4) after preincubation was added and again incubated at 30°C. The absorbances were spectrophotometrically measured at 405 nm, according to previous studies.[18,38–40]

4.3 | In silico studies

Druglikeness properties of all novel compounds and inhibition mechanism of compounds, which have the best inhibition score against α-glycosidase receptor, were calculated and specified with in silico methods. The Small Drug Discovery Suites package (Schrödinger 2019-3 LLC) was used in performing in silico studies.[41–43]

4.3.1 | Ligand preparation and pharmacokinetic properties prediction

For the QikProb and induced-fit docking studies, 2D structure of the compounds with best inhibition score was sketched and their 3D structure was produced with LigPrep module of Schrodinger Maestro 12.0. Correct molecular geometries and protonation state at pH 7.0 ± 2.0 of ligand were prepared using Epik module and OPLS-2005 force field.[44,45] The pharmacokinetic properties of prepared ligands were calculated with QikProp module of Schrodinger Maestro 12.0. Briefly, prepared ligands were opened and the calculation was performed using the default parameter by selecting the five most similar drug molecule options on QikProp module.[46,47]

4.3.2 | Protein preparation and binding site prediction

X-ray crystal structures of *S. cerevisiae* α-glycosidase receptor (PDB code: 3A4A) and human lysosomal α-glycosidase (PDB code: 5NN8) have been acquired from RCSB Protein Data Bank. They have been selected due to their best resolution and good percentile ranks. Moreover, the structures have a ligand which can be used for docking validation test in the catalytic active site. The typical crystal structure

in the PDB format is not suitable for immediate use in molecular modeling calculations. Hence, the crystal structure has been repaired and prepared with protein preparation wizard module of Schrodinger Maestro 12.0 before using in binding site prediction and induced-fit docking studies. The workflow that includes a detailed description of previous studies[48,49] was described in the overview. Bond order and charges were assigned and then missing hydrogen atoms were added to crystal structure. Missing side chains were filled using Prime module of the program. Amino acids were ionized by setting physiological pH with the help of Propka software. Water molecules that formed less than three contacts with the protein or ligand were removed. Finally, energy minimization and geometry optimization have also been performed using OPLS force field.

After protein preparation, the catalytic site of the receptors was predicted with SiteMap module of Schrodinger Maestro 12.0 for target selection and docking hits' evaluation. The prepared receptor was imported into Maestro 12.0, and the binding site was predicted using the default parameter of top-ranked potential protein binding site. The analysis of SiteScore and DScore determined whether the binding site had catalytic active site characteristics.[50,51]

4.3.3 | Induced-fit docking

To determine binding affinities and inhibition mechanisms of the compounds with the best inhibition score, molecular docking studies were carried out. Induced-fit docking technique is one of the best ways to calculate binding affinity between ligand and receptor, because both ligand and receptor are completely flexible in this docking technique. The technique has been performed with the induced-fit docking module of Schrodinger Maestro 12.0 according to proposed previous studies.[52–54] The centroid of the residues was generated around the selected ligand or residues in the catalytic site of the receptor. Then, side chains were automatically trimmed based on B-factor; the closest residues to the ligand were refined within 3.4 Å of ligand pose in prime refinement. Before calculating binding affinity between ligands and the receptors, docking validation test was carried out for understanding accuracy of induced-fit docking technique. The test has been performed with redocking procedure by evicting inhibitor complexed in the crystal structure of the receptors. The RMSD value between cocrystallized ligand and redocked ligand has been calculated with the atom pair method in Superposition panel of Schrodinger Maestro 12.0. Following the docking process, best-scored compounds have been determined by analyzing docking scores.

CONFLICTS OF INTEREST

The authors declare that there are no conflicts of interests.

ORCID

Parham Taslimi http://orcid.org/0000-0002-3171-0633
Muhammet Karaman http://orcid.org/0000-0002-0155-3390

REFERENCES

[1] B. Jank, T. Pernat, C. O. Kappe, *Molecules* **2000**, *5*, 227.
[2] I. S. Zorkun, S. Sarac, S. Celebi, K. Erol, *Bioorg. Med. Chem.* **2006**, *16*, 4479.
[3] J. J. V. Eynde, N. Audiort, V. Canonne, S. Michel, Y. V. Haverbeke, C. O. Kappe, *Heterocycles* **1997**, *45*, 1967.
[4] D. Dalinger, A. Stadler, C. O, *Pure Appl. Chem.* **2004**, *76*, 1017.
[5] A. Sujayev, E. Garibov, *Organic Chemistry*, Lambert Academic Publishing, Germany **2016**, p. 55.
[6] S. A. Sardarova, S. F. Osmanova, F. A. Mamedov, Sh. Y. Gamidova, *Chem. Probl.* **2015**, *3*, 319.
[7] P. P. Ashvini, K. P. Tejasvi, R. P. Ankita, *World J. Pharm. Pharm. Sci.* **2015**, *4*, 1780.
[8] H. K. Nisreen, H. T. Jumbad, H. Ammar, Al Ibn Al-Haitham, *J. Pure Appl. Sci.* **2013**, *26*, 296.
[9] A. Ricci, *Angew. Chem., Int. Ed. Engl.* **2007**, *5*, 22.
[10] I. Gulcin, A. Z. Tel, A. C. Gören, P. Taslimi, S. Alwasel, *J. Food Meas. Charact.* **2019**, *13*, 2062.
[11] P. Taslimi, F. M. Kandemir, Y. Demir, M. İleritürk, Y. Temel, C. Cağlayan, I. Gulcin, *J. Biochem. Mol. Toxicol.* **2019**, *33*, e22313.
[12] H. Genc Bilgicli, A. Kestane, P. Taslimi, O. Karabay, A. Bytyqi-Damoni, M. Zengin, I. Gulcin, *Bioorg. Chem.* **2019**, *88*, 102931.
[13] R. Kaya, P. Taslimi, M. E. Naldan, I. Gulcin, *Lett. Drug Des. Discov* **2019**, *14*, 573.
[14] E. Bursal, A. Aras, Ö. Kılıç, P. Taslimi, A. C. Gören, I. Gulcin, *J. Food Biochem.* **2019**, *43*, e12776.
[15] V. Farzaliyev, P. Taslimi, A. Sujayev, N. Nazarov, Z. Huyut, S. H. Alwasel, I. Gulcin, *J. Biochem. Mol. Toxicol.* **2017**, *31*, e21897. https://doi.org/10.1002/jbt.21897
[16] P. Taslimi, A. Sujayev, F. Turkan, E. Garibov, Z. Huyut, V. Farzaliyev, S. Mamedova, I. Gulcin, *J. Biochem. Mol. Toxicol.* **2018**, *32*, e22019. https://doi.org/10.1002/jbt.22019
[17] P. Taslimi, S. Osmanova, C. Caglayan, F. Turkan, S. Sardarova, V. Farzaliyev, A. Sujayev, N. Sadeghian, I. Gulcin, *J. Biochem. Mol. Toxicol.* **2018**, *32*, e22191. https://doi.org/10.1002/jbt.22191
[18] Y. Tao, Y. Zhang, Y. Cheng, Y. Wang, *Biomed. Chromatogr.* **2013**, *27*, 148.
[19] Y. Natori, T. Imahori, Y. Yoshimura, *J. Synth. Org. Chem., Jpn.* **2016**, *74*, 335.
[20] A. Aktas, D. Barut Celepci, Y. Gok, P. Taslimi, H. Akıncioglu, I. Gulcin, *Crystals* **2020**, *10*, 171.
[21] A. Maharramov, R. Kaya, P. Taslimi, M. Kurbanova, A. Sadigova, V. Farzaliyev, A. Sujayev, I. Gulcin, *Arch. Pharm.* **2019**, *352*, e1800317.
[22] P. Taslimi, H. E. Aslan, Y. Demir, N. Oztaskin, A. Maraş, I. Gulcin, S. Beydemir, S. Goksu, *Int. J. Biol. Macromol.* **2018**, *119*, 857.
[23] M. Huseynova, P. Taslimi, A. Medjidov, V. Farzaliyev, M. Aliyeva, G. Gondolova, O. Şahin, B. Yalçın, A. Sujayev, E. B. Orman, A. R. Özkaya, I. Gulcin, *Polyhedron* **2018**, *155*, 25.
[24] M. Zengin, H. Genc, P. Taslimi, A. Kestane, E. Guclu, A. Ogutlu, O. Karabay, I. Gulcin, *Bioorg. Chem.* **2018**, *81*, 119.
[25] I. Gulcin, P. Taslimi, A. Aygün, N. Sadeghian, E. Bastem, O. I. Kufrevioglu, F. Turkan, F. Şen, *Int. J. Biol. Macromol.* **2018**, *119*, 741.
[26] K. Yamamoto, H. Miyake, M. Kusunoki, S. Osaki, *FEBS J.* **2010**, *277*, 4205.
[27] K. Yamamoto, H. Miyake, M. Kusunoki, S. Osaki, *J. Biosci. Bioeng.* **2011**, *112*, 545.
[28] L. Suresh, P. Onkara, P. S. V. Kumar, Y. Pydisetty, G. V. P. Chandramouli, *Bioorg. Med. Chem. Lett.* **2016**, *26*, 4007.
[29] A. Barakat, S. M. Soliman, A. M. Al-Majid, G. Lotfy, H. A. Ghabbour, H. Fun, S. Yousuf, M. I. Choudhary, A. Wadood, *J. Mol. Struct.* **2015**, *1098*, 365.
[30] A. Ibrar, S. Zaib, I. Khan, Z. Shafique, A. Saeed, J. Iqbal, *J. Taiwan Inst. Chem. Eng.* **2017**, *81*, 119.
[31] M. Saeedi, M. Mohammadi-Khanposhtani, M. S. Asgari, N. Eghbalnejad, S. Imanparast, M. A. Faramarzi, B. Larijani, M. Mahdavi, T. Akbarzadeh, *Bioorg. Med. Chem. Lett.* **2019**, *27*, 115148.

[32] V. Roig-Zamboni, B. Cobucci-Ponzano, R. Iacono, M. C. Ferrara, S. Germany, Y. Bourne, G. Parenti, M. Moracci, G. Sulzenbacher, *Nat. Commun.* **2017**, *8*, 1111.
[33] S. Taj, U. A. Ashfaq, S. Aslam, M. Ahmad, S. H. Bhatti, *Biologia* **2019**, *74*, 1523.
[34] B. Yiğit, R. Kaya, P. Taslimi, Y. Işık, M. Karaman, M. Yiğit, İ. Özdemir, I. Gulcin, *J. Mol. Struct.* **2018**, *1179*, 709.
[35] P. Taslimi, E. Koksal, A. C. Gören, E. Bursal, A. Aras, O. Kılıç, S. Alwasel, I. Gulcin, *Arab. J. Chem.* **2020**, *13*, 4528.
[36] S. Burmaoğlu, E. Akın Kazancioglu, R. Kaya, M. Kazancioglu, M. Karaman, O. Algül, I. Gulcin, *J. Mol. Struct.* **2020**, *1208*, 127868.
[37] P. Taslimi, K. Turhan, F. Turkan, H. S. Karaman, Z. Turgut, I. Gulcin, *Bioorg. Chem.* **2020**, *97*, 103647.
[38] C. Çaglayan, Y. Demir, S. Kucukler, P. Taslimi, F. M. Kandemir, I. Gulcin, *J. Food Biochem.* **2019**, *43*, e12720.
[39] N. Eruygur, M. Ataş, M. Tekin, P. Taslimi, U. M. Koçyiğit, I. Gulcin, *S. Afr. J. Bot.* **2019**, *120*, 141.
[40] Y. Demir, P. Taslimi, M. S. Ozaslan, N. Oztaskin, Y. Çetinkaya, I. Gulcin, Ş. Beydemir, S. Goksu, *Arch. Pharm.* **2018**, *351*, 1800263.
[41] Z. Koksal, R. Kalın, P. Kalın, M. Karaman, I. Gulcin, H. Ozdemir, *J. Food Biochem.* **2020**, *44*, e13132.
[42] M. Yigit, B. Yigit, P. Taslimi, I. Ozdemir, M. Karaman, I. Gulcin, *J. Mol. Struct.* **2020**, *1207*, 127802.
[43] S. Bal, R. Kaya, P. Taslimi, A. Aktas, M. Karaman, I. Gulcin, *Bioorg. Chem.* **2020**, *94*, 103468.
[44] C. Bayrak, P. Taslimi, H. S. Kahraman, I. Gulcin, A. Menzek, *Bioorg. Chem.* **2019**, *85*, 128.
[45] LigPrep, Schrödinger, LLC, New York, NY **2019**.
[46] QikProp, Schrödinger, LLC, New York, NY **2019**.
[47] F. Turkan, A. Cetin, P. Taslimi, H. S. Karaman, I. Gulcin, *Arch. Pharm.* **2019**, *352*, e1800359.
[48] U. Atmaca, R. Kaya, H. S. Kahraman, M. Celik, I. Gulcin, *Bioorg. Chem.* **2019**, *88*, 102980.
[49] P. Taslimi, F. Turkan, A. Cetin, H. Burhan, M. Karaman, I. Bildirici, I. Gulcin, F. Sen, *Bioorg. Chem.* **2019**, *92*, 103213.
[50] SiteMap, Schrödinger, LLC, New York, NY **2019**.
[51] S. Bayindir, C. Caglayan, M. Karaman, I. Gulcin, *Bioorg. Chem.* **2019**, *90*, 103096.
[52] (a) Induced Fit Docking protocol, Glide, Schrödinger, LLC, New York, NY 2016. (b) Prime, Schrödinger, LLC, New York, NY 2019.
[53] F. Turkan, A. Cetin, P. Taslimi, M. Karaman, I. Gulcin, *Bioorg. Chem.* **2019**, *86*, 420.
[54] R. Kalin, Z. Koksal, P. Kalin, M. Karaman, I. Gulcin, H. Ozdemir, *J. Biochem. Mol. Toxicol.* **2020**, *34*, e22421.

SUPPORTING INFORMATION

Additional supporting information may be found online in the Supporting Information section.

How to cite this article: Taslimi P, Sujayev A, Karaman M, et al. *N*-Substituted pyrimidinethione and acetophenone derivatives as a new therapeutic approach in diabetes. *Arch Pharm*. 2020;e2000075.
https://doi.org/10.1002/ardp.202000075